J Physiol 588.6 (2010) pp 907–922

The Journal of Physiology

Reduced expression of the Ca^{2+} transporter protein PMCA2 slows Ca^{2+} dynamics in mouse cerebellar Purkinje neurones and alters the precision of motor coordination

Ruth M. Empson[1,3], Paul R. Turner[1], Raghavendra Y. Nagaraja[1], Philip W. Beesley[2] and Thomas Knöpfel[3]

[1] *Department of Physiology, University of Otago School of Medical Sciences, Dunedin, New Zealand*
[2] *School of Biological Sciences, Royal Holloway University of London, Egham, Surrey, TW20 0EX, UK*
[3] *Laboratory for Neuronal Circuit Dynamics, RIKEN Brain Science Institute, Wako-ishi, Saitama, 351-0198, Japan*

Cerebellar Purkinje neurones (PNs) express high levels of the plasma membrane calcium ATPase, PMCA2, a transporter protein critical for the clearance of calcium from excitable cells. Genetic deletion of one PMCA2 encoding gene in heterozygous PMCA2 knock-out ($PMCA2^{+/-}$) mice enabled us to determine how PMCA2 influences PN calcium regulation without the complication of the severe morphological changes associated with complete PMCA2 knock-out ($PMCA2^{-/-}$) in these cells. The $PMCA2^{+/-}$ cerebellum expressed half the normal levels of PMCA2 and this nearly doubled the time taken for PN dendritic calcium transients to recover (mean fast and slow recovery times increased from 70 ms to 110 ms and from 600 ms to 1100 ms). The slower calcium recovery had distinct consequences for $PMCA2^{+/-}$ PN physiology. The PNs exhibited weaker climbing fibre responses, prolonged outward Ca^{2+}-dependent K^+ current (mean fast and slow recovery times increased from 136 ms to 192 ms and from 595 ms to 1423 ms) and a slower mean frequency of action potential firing (7.4 Hz compared with 15.8 Hz). Our findings were consistent with prolonged calcium accumulation in the cytosol of $PMCA2^{+/-}$ Purkinje neurones. Although $PMCA2^{+/-}$ mice exhibited outwardly normal behaviour and little change in their gait pattern, when challenged to run on a narrow beam they exhibited clear deficits in hindlimb coordination. Training improved the motor performance of both $PMCA2^{+/-}$ and wild-type mice, although $PMCA2^{+/-}$ mice were always impaired. We conclude that reduced calcium clearance perturbs calcium dynamics in PN dendrites and that this is sufficient to disrupt the accuracy of cerebellar processing and motor coordination.

(Received 8 October 2009; accepted after revision 13 January 2010; first published online 18 January 2010)
Corresponding author R. M. Empson: University of Otago, Physiology, 270 Great King Street, Dunedin 9001, New Zealand. Email: ruth.empson@stonebow.otago.ac.nz

Abbreviations CF, climbing fibre; FGF-14, fibroblast growth factor 14; LTD, long-term depression; OGB-1, Oregon Green BAPTA 1; PMCA2, plasma membrane Ca^{2+}-ATPase isoform 2; PN, Purkinje neurone; SERCA, sarcoplasmic endoplasmic reticulum Ca^{2+}-ATPase.

Introduction

The stringent control of intracellular calcium levels $[Ca^{2+}]_i$ in neurones is necessary both for their survival and their calcium-dependent electrical signalling. Control is achieved by a delicate balance between Ca^{2+} 'on' and 'off' mechanisms, elegantly described as the calcium signalling toolkit (Berridge *et al.* 2003). One of the 'off' mechanisms is the plasma membrane Ca^{2+}-ATPase (PMCA), a family of P-type Ca^{2+}-ATPases that clear Ca^{2+} from the cytosol using energy derived from ATP (Carafoli, 1992; Strehler & Zacharias, 2001). Their high affinity for Ca^{2+} makes them a very effective Ca^{2+} recovery mechanism during $[Ca^{2+}]_i$ transients but also at $[Ca^{2+}]_i$ close to rest (Thayer *et al.* 2002). Of the four PMCA isoforms, PMCAs 2 and 3 are enriched within excitable cells where their fast activation and clearance rates (Brini *et al.* 2003) are well suited to control fast neuronal $[Ca^{2+}]_i$ dynamics.

In the rat brain, the expression of PMCA2 is highest in the cerebellum where it is enriched within the main output neurones of the cerebellum, the Purkinje neurones (PNs) (Filoteo *et al.* 1997; Burette *et al.* 2003). The contribution of PMCA2 to cerebellar function is evident from the phenotype of PMCA2 knockout mice, but the mechanisms are unclear. In addition to hearing loss and vestibular abnormalities these mice are severely ataxic,

© 2010 The Authors. Journal compilation © 2010 The Physiological Society
DOI: 10.1113/jphysiol.2009.182196

their cerebellar cortex is reduced in thickness (Kozel *et al.* 1998) and PN dendrites are stunted and disordered (Empson *et al.* 2007).

As a critical component of cerebellar function, the PN receives a powerful synaptic, glutamatergic input from the inferior olive, called the climbing fibre (CF). The PN response to CF input, often called the complex spike (Eccles *et al.* 1966), is accompanied by a large rise in cytosolic $[Ca^{2+}]_i$ (Knöpfel *et al.* 1991; Miyakawa *et al.* 1992). This calcium rise contributes to the induction of long-term depression (LTD) of coincidentally activated parallel fibre synapses (Ito & Kano, 1982) and the CF response itself (Hansel & Linden, 2000). Together these important forms of synaptic plasticity are thought to convey cerebellar motor learning signals (Ito, 2006) and as is expected, disruption of PN calcium homeostasis disrupts cerebellar functions. Thus, in mice with a null mutation of the PN calcium buffer calbindin, an important Ca^{2+} 'off' mechanism, PN calcium homeostasis is disrupted and the mice exhibit ataxia (Airaksinen *et al.* 1997; Barski *et al.* 2003). Conversely, mutations or loss of PN P/Q-type voltage-gated calcium channels, a Ca^{2+} 'on' mechanism, in EA2 (episodic ataxia) *ducky* and *staggerer* mice decreases the precision of PN firing, eliminates calcium spikes and also results in ataxia (Crepel *et al.* 1984; Walter *et al.* 2006; Donato *et al.* 2006).

Here we show that PMCA2, an active Ca^{2+} 'off' mechanism, is also required for normal cerebellar function. We took advantage of mice lacking one allele for PMCA2 ($PMCA2^{+/-}$ mice) where the cerebellar PNs did not exhibit any obvious structural abnormalities but expressed half the wild-type levels of PMCA2. As a result, calcium dynamics in $PMCA2^{+/-}$ PN dendrites were perturbed and this in turn reduced CF responses and slowed action potential firing frequency. Furthermore, the $PMCA2^{+/-}$ mice lacked coordination on a narrow beam test although their running gait was normal. Together our results identify the importance of finely tuned PMCA2-mediated calcium recovery in PN dendrites for the accuracy of cerebellar processing and motor coordination.

Methods

Ethical approval

All animal husbandry and procedures minimized animal suffering and were carried out using internationally recognized standards approved by RIKEN BSI, Tokyo, Japan and by the University of Otago, Dunedin, New Zealand Animal Ethics Committee working to the New Zealand Animal Welfare Act (1999). All our experiments comply with the policies and regulations described in Drummond, 2009.

Mice

PMCA2 knockout mice were a generous gift from Dr Gary Shull (Kozel *et al.* 1998) and were maintained as two colonies based upon FVBN and Swiss B6 background strains both in Japan and New Zealand. Both strains were used interchangeably throughout the study without any detectable differences, unless where stated. The genotype of each mouse was determined, pre-weaning as previously described (Empson *et al.* 2007).

Electrophysiology

Sagittal slices, 270 μm thick, were prepared from age-matched littermate mice (sometimes on the same day), approximately 4 weeks old, following rapid terminal anaesthesia with halothane or carbon dioxide (Empson *et al.* 2007). Slices were maintained at 24°C (TC324B, Harvard Apparatus, USA) in a flow (3 ml min^{-1}) of artificial cerebrospinal fluid (aCSF), equilibrated with 95% O_2 and 5% CO_2, containing (in mM): NaCl 126, KCl 2.5, NaH_2PO_4 1.2, $MgCl_2$ 1.3, $CaCl_2$ 2.4, $NaHCO_3$ 26, glucose 10. Whole cell recordings from PN soma under visual control used glass electrodes (3–4 MΩ) containing (in mM): KCl 5, KOH 20, $MgCl_2$ 3.48, NaCl 4, potassium gluconate 120, Hepes 10, sucrose 18, Na_2ATP 4, Na_3GTP 0.4, and for simultaneous imaging 100 μM Oregon Green BAPTA-1 (OGB-1), or 10 mM EGTA replacing sucrose when strong buffering of PN $[Ca^{2+}]_i$ was required, pH 7.3 and osmolarity 305 mosmol l^{-1}. Voltage clamp (Axopatch 200B or, in some cells, Axoclamp 2A, Molecular Devices, USA) maintained cells at –65 mV with typically less than −0.2 nA holding current for at least 10 min prior to electrophysiological protocols. Series resistances were typically 12–20 MΩ and no greater than 30 MΩ. Input resistances, with a mean of approximately 125 MΩ, were similar for wild-type and $PMCA2^{+/-}$ Purkinje neurones ($P = 0.55$, t test). Their mean membrane potential, recorded in current clamp, was approximately −50 mV and also similar between the two groups ($P = 0.48$, t test). Complex spike inward currents (and potentials, in some cells) were evoked following CF stimulation (approx. 2–15 μA or 0–20 V) at 0.011 Hz (every 90 s) using a glass aCSF-filled electrode (200–600 kΩ) placed in the granule cell layer approximately 50 μm from the recorded cell. Climbing fibre-induced responses exhibited an all-or-none character. Depolarization-induced calcium responses and outward currents were evoked, also at 0.011 Hz, in voltage clamp by depolarizing the PN from a holding potential of −80 mV to 0 mV for a period of 400 ms (Fierro *et al.* 1998).

Pipettes used to make extracellular recordings under visual control were of similar resistance to those used for whole-cell patch clamping but contained aCSF. Spontaneous firing of PN action potentials was best

© 2010 The Authors. Journal compilation © 2010 The Physiological Society

recorded towards the axon hillock region of the cell and recordings typically lasted up to 20 min. All offline analysis used pCLAMP 9 (Molecular Devices, USA). A total of 38 mice (24 also used in the imaging experiments below) were used for electrophysiological analysis.

Calcium imaging

At least 25 min was allowed after whole-cell patch clamp to permit sufficient Oregon Green BAPTA-1 (OGB-1) to diffuse into the PN dendrites. A set of dendrites was selected for imaging using the frame mode of the upright D-Eclipse C1 confocal laser scanning microscope equipped with a ×60 water immersion objective. Excitation wavelength was 488 nm and fluorescence was sampled through a 530 ± 15 nm band pass filter. Ca^{2+} transients were acquired in linescan mode at a nominal x-resolution of 4.8 pixels per micrometre. Fluorescence, electrophysiological recordings and electrophysiological stimulation was synchronized using a Master 8 (AMPI, Israel). Linescans were repeated 3–5 times to generate averaged linescan x–t images captured at 16 bit. Laser power and photomultiplier settings were kept consistent between experiments while keeping basal fluorescence levels typically at less than one-quarter of the dynamic range; we observed no difference in the required laser power or photomultiplier (PMT) settings, when recording from $PMCA2^{+/+}$ and $PMCA2^{+/-}$ PNs (mean values were $6.5 \pm 0.4\%$ and $6.5 \pm 0.5\%$ for laser power, and 102 ± 1.2 and 103 ± 0.6 for PMT settings, $n = 16$ and 20, respectively), but did observe slightly raised baseline fluorescence counts in $PMCA2^{+/-}$ PNs. We kept the calcium indicator concentration consistent throughout the experiments by carefully controlling both the time of recording after attaining whole cell (and therefore the time allowed for diffusion of indicator) and the distance from the soma where the recordings were made. Comparisons between $PMCA2^{+/+}$ and $PMCA2^{+/-}$ PN recordings revealed no significant differences; measurements were made 34.6 ± 1.6 and 36.7 ± 2.3 min, respectively, after whole cell ($P = 0.47$, t test) at a distance of 78.9 ± 7.5 and 72.3 ± 5.3 μm, respectively ($P = 0.48$, t test), and from dendrites of a similar thickness 2.14 ± 0.07 and 2.19 ± 0.08 μm, respectively ($P = 0.62$, t test). In all cells, analysis of the change in fluorescence in each dendrite over time was extracted from linescan x–t images using ImagePro (Media Cybernetics Inc., USA). In most cases, further sets of dendrites were recorded from different parts of the same cell. At the laser intensities employed, fluorescence bleaching was negligible so signals were not corrected for dye bleaching. At the end of each imaging experiment a full z-stack of the cell was collected using a step size of 1.5 μm and each cell reconstructed (ImageJ, http://rsbweb.nih.gov/ij/) to identify the location of dendrites for analysis and to determine any major structural differences between PNs. Twenty-four mice were used for calcium-imaging analysis.

Western blotting

To prepare homogenates, the cerebella of $PMCA2^{+/+}$, $PMCA2^{+/-}$ and $PMCA2^{-/-}$ mice, 4–6 weeks old, were removed into RIPA buffer, pH 7.4 (Sigma-Aldrich, New Zealand), containing protease inhibitors (Roche, New Zealand) and homogenized. SDS-PAGE on 15% acrylamide Tris-glycine gels (BioRad, New Zealand) was used to separate 60 μg protein. Transferred proteins were probed using primary antibodies specific for the N-terminal epitope of PMCA2 (NR2, Abcam, UK), calbindin (Abcam) and tubulin (mouse monoclonal, Sigma-Aldrich) as a loading control. A Bio-Rad model GS-700 imaging densitometer was used to quantify band density with Quantity One v.4.6.3 software and values expressed as band optical density × mm^2 normalized to tubulin optical density. Eighteen mice were used for protein analysis.

Fluorescence-based immunohistochemistry

Groups of three $PMCA2^{+/+}$, $PMCA2^{+/-}$ and $PMCA2^{-/-}$ mice, approximately 4 weeks old, were heavily anaesthetized (as assessed by lack of paw withdrawal in response to pressure) using an intraperitoneal injection of a mixture of ketamine (300 mg kg^{-1}) and xylazine (30 mg kg^{-1}). Mice were then transcardially perfused with ice-cold phosphate-buffered saline (PBS) containing 4% paraformaldehyde after which the brains were stored in PBS. Sagittal slices (30 μm thick) were cut from the cerebella using a freezing sledge microtome (Leitz, Westlar, Germany). The slices were processed as previously described (Jensen *et al.* 2007) and viewed with a ×40 air and ×100 oil immersion objective on an upright fluorescence microscope (Olympus model BX50, Olympus New Zealand). Images were collected with an F-view CCD camera (Olympus Soft Imaging System) controlled by Olympus CellP software using similar exposure times and filter settings between slices from the different mice. Nine mice were used for immunohistochemistry.

Behavioural tests

Two behavioural tests were used in this study, a simple and sensitive beam-walking test and Catwalk, a computer-assisted gait analysis hardware and software (Noldus Inc., The Netherlands). Mice for behavioural analysis were obtained by $PMCA2^{+/+}$ and $PMCA2^{+/-}$ crosses to generate an equal number of $PMCA2^{+/+}$ or

© 2010 The Authors. Journal compilation © 2010 The Physiological Society

PMCA2$^{+/-}$ offspring. We restricted our experiments to both male and female FVBN mice since they were active and compliant on the beam test compared with age- and genotype-matched B6 mice. The latter were slow on the beam and often refused to cross it at all whether wild-type or heterozygous, and this made the test impossible to perform. As described above, mice were genotyped prior to weaning and then housed in their experimental groups before use at approximately 4 weeks of age. Two days before the tests, and on each test day, the mice were handled and weighed. Handling and tests took place under conditions of sodium lighting (McLennan & Taylor-Jeffs, 2004) at the same time each day that mimicked early dusk.

Beam balance test. Testing was conducted in a random order each day and video-captured for off-line analysis; the experimenters were blind to the mouse genotype at all times. The custom-made Plexiglas beam was 1 cm wide, 1 m long and at a height of 10 cm. Mice were placed on the beam at one of either end (random choice) and traversed the beam spontaneously. Each mouse received five trials on the beam, with approximately 30 s between trials, before it was returned to a holding cage. Mice were tested on 5 consecutive days and then allowed a 2 day rest period before a final 6th test on day 8. One month later mice were re-tested on the beam using the same protocol. Off-line analysis counted the number of hindlimb slips made by each mouse per trial and the average number of slips per meter calculated for each trial. The time for each mouse to traverse the beam was also measured, removing any times when the mouse was stationary on the beam, and measurements compared on day 5 of the trial. None of the mice fell from the beam.

Gait analysis with Catwalk. Mice received up to five trials on a gait analysis smooth glass runway, Catwalk (Noldus Inc., The Netherlands), to assess any differences in their unchallenged gait, either before or after their beam test. Twenty-nine mice were used for behavioural analysis.

Statistics

Prism 3.03 (Graphpad Software) calculated the mean and standard error of the mean (S.E.M.) and statistical comparisons using either one- or two-way ANOVA where appropriate using Bonferroni *post hoc* comparisons, or paired or unpaired Student's *t* test where appropriate. Origin software (OriginLab, USA) was used for the exponential unconstrained fits of calcium transients, pCLAMP 9 for the exponential unconstrained fits of outward currents.

Results

PMCA2 expression levels

As shown in Fig. 1*A*, calbindin expression revealed the shape and extent of the PNs throughout the cerebellar cortex to be very similar for wild-type and heterozygous PMCA2 knockout (PMCA2$^{+/-}$) mice. In contrast, calbindin labelling of the cerebellar cortex from homozygous PMCA2 knockout (PMCA2$^{-/-}$) mice (Fig. 1) confirmed our previous observation that PNs completely lacking PMCA2 exhibited very distorted and stunted dendrites (Empson *et al.* 2007) consistent with the thinner cerebellar cortex (Kozel *et al.* 1998). In contrast, the extent of the dendrites of individually reconstructed PNs from the PMCA2$^{+/-}$ mice was very similar to wild-type PMCA2$^{+/+}$ cells ($P = 0.3$, dendrite width, $P = 0.61$, dendrite length, *t* tests, $n = 8$).

As expected, PMCA2 expression was not detectable in the PMCA2$^{-/-}$ cerebellar cortex but was observed in the PMCA2$^{+/-}$ cerebellar Purkinje neurones, with no sign of a mosaic (Fig. 1*A* middle panel) and more distinctively within the somatic and dendritic membranes, including the spines of the Purkinje neurones in the wild-type PMCA2$^{+/+}$ cerebellar cortex (Fig. 1*A*, left panel, inset). Semi-quantitative Western blots confirmed that PMCA2 expression was significantly reduced in the PMCA2$^{+/-}$ cerebellum to approximately half that observed in wild-type mice (see Fig. 1*B*) and accords with a previous study (Kozel *et al.* 1998) where mRNA for PMCA2 was reduced in the PMCA2$^{+/-}$ mouse. Mean values of PMCA2 protein band density normalized to tubulin band density were reduced from 7.1 ± 0.8 in the wild-type to 3.5 ± 0.5 in the PMCA2$^{+/-}$ heterozygous mouse, whilst PMCA2$^{-/-}$ tissue did not contain any detectable PMCA2 protein at all ($P < 0.0001$, one-way ANOVA, $n = 5$). However, in contrast to a previous study (Hu *et al.* 2006) we could not detect any significant alterations to the expression of the calcium-binding protein calbindin in PMCA2$^{+/-}$ or PMCA2$^{-/-}$ cerebellum (see Fig. 1*B*; $P = 0.44$, one-way ANOVA, $n = 6$).

Recovery of climbing fibre-evoked dendritic calcium transients

We were therefore able to take advantage of the intact morphology of the PMCA2$^{+/-}$ PN dendrites and their reduced PMCA2 expression to examine how PMCA2 contributes to calcium dynamics in these cells. As shown in Fig. 2, we challenged the PNs with a calcium load evoked by electrical activation of their climbing fibre (CF) input. Fast linescan-based measurements from their proximal dendrites, filled with OGB-1 (see Fig. 2*A*) revealed a large, rapid rise in the fluorescence intensity, coincident with the stimulus-evoked CF response (top trace) that

© 2010 The Authors. Journal compilation © 2010 The Physiological Society

then recovered with a time course best fitted with a double exponential (see Fig. 2*B*) to reveal two decay time constants. Fluorescence-based calcium responses from PMCA2$^{+/+}$ PN dendrites were very similar to previously reported values (Lev-Ram *et al.* 1992; Eilers *et al.* 1995; Airaksinen *et al.* 1997; Schmidt *et al.* 2003), both in their peak amplitude, represented as $\%\Delta F/F$, (change in fluorescence over baseline fluorescence) and in their fast and slow decay time constants. However, in PMCA2$^{+/-}$ PN dendrites both decay time constants were significantly prolonged, indicative of slowed calcium clearance from the dendrites and consistent with the reduced expression of PMCA2 (see Fig. 1*A*). The first decay time constant of the recovery of the CF-induced calcium response was significantly prolonged from 69.7 ± 6.2 ms ($n = 87$ dendrites from 10 cells) in the wild-type PMCA2$^{+/+}$ PN dendrites to 110.5 ± 10.9 ms in the PMCA2$^{+/-}$ dendrites ($n = 137$ from 12 cells, $P < 0.001$, *t* test). The second decay time constant of CF-induced fluorescence recovery was also prolonged from 613.7 ± 24.3 ms in wild-type to 1111 ± 52.1 ms in PMCA2$^{+/-}$ dendrites ($P < 0.001$, one-way ANOVA multiple comparison). CF-induced calcium transients from PMCA2$^{-/-}$ PN dendrites were very abnormal and often failed to recover (data not shown).

These findings indicate that during CF-induced calcium rises in PN dendrites a PMCA2-mediated calcium clearance mechanism provides for fast and effective return of elevated calcium concentrations back to their resting levels.

We noted that the peak amplitude $\%\Delta F/F$ of the CF-induced calcium response, as shown in Fig. 2*B*, was also reduced in the PMCA2$^{+/-}$ PNs compared with wild-type. Mean $\%\Delta F/F$ changed from 44 ± 2.2 in PMCA2$^{+/+}$ PNs to 31.1 ± 1.9 in PMCA2$^{+/-}$ PNs ($P < 0.001$, *t* test).

Part of the explanation for the reduced amplitude of the CF-induced calcium response in the PMCA2$^{+/-}$ PNs was their weaker electrophysiological response to climbing fibre activation (Fig. 2). Mean values for the amplitude of the CF-induced inward current were reduced by around 20% in PMCA2$^{+/-}$ PNs, from 1502 ± 128 pA in wild-type PNs to 1179 ± 89 pA, $P < 0.05$, *t* test, $n = 12$. Along with

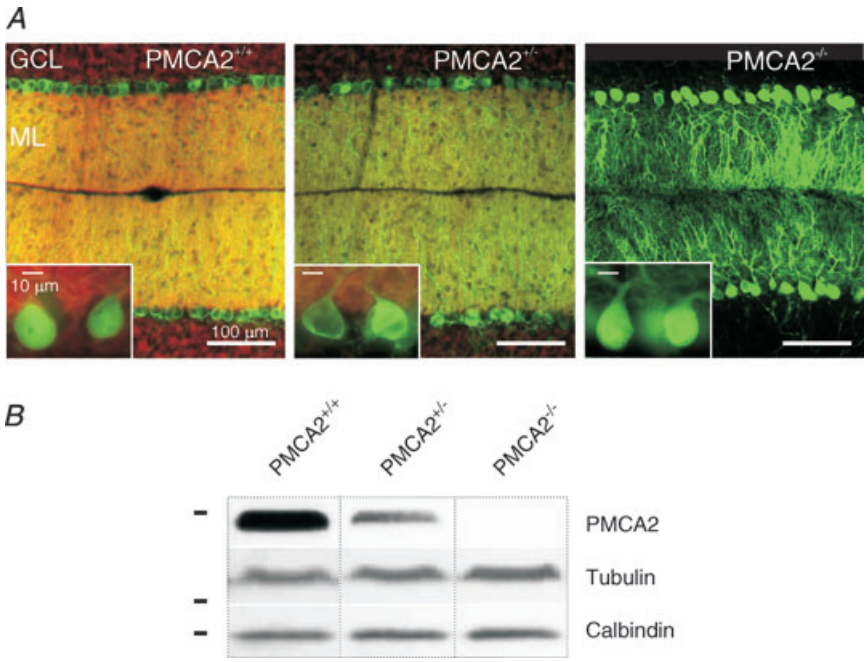

Figure 1. PMCA2 expression is approximately halved in PMCA2$^{+/-}$ mouse cerebellum with little change in gross structure of the cerebellum or PNs

A, sagittal sections from mouse cerebellum labelled with calbindin (green) and PMCA2 (red) in wild-type PMCA2$^{+/+}$, heterozygous PMCA2$^{+/-}$ and homozygous knockout PMCA2$^{-/-}$ mice granule cell (GCL) and molecular layers (ML). The insets show a higher resolution image of Purkinje neurone soma where the characteristic plasma membrane location of the PMCA2 is visible in PMCA2$^{+/+}$ PNs. PMCA2 was still detectable by immunohistochemistry in the PMCA2$^{+/-}$ cerebellum but less than wild-type expression, and as expected not detectable at all in PMCA2$^{-/-}$ cerebellum. Calbindin was present in all PN dendrites and shows the stunted and disordered structure of the PMCA2$^{-/-}$ PN dendrites (see right-hand panel). Camera and filter settings were identical between sections for both fluorophores. *B*, semi-quantitative Western blotting shows PMCA2 expression to be approximately halved in the PMCA2$^{+/-}$ mouse cerebellum, as indicated by a representative blot in the top panel, where calbindin expression and tubulin expression as loading controls are shown for the same samples, from the same blot and film. Horizontal bars represent the positions of molecular mass markers at 198.4, 38.2 and 31.3 kDa.

© 2010 The Authors. Journal compilation © 2010 The Physiological Society

this alteration in current amplitude, we observed a reduced number of CF-evoked spikelets in the PMCA2$^{+/-}$ PNs, as is also evident in the example shown in Fig. 2*B*; the mean number of spikelets per CF response measured in voltage clamp, changed from 3.7 ± 0.3 in the PMCA2$^{+/+}$ PNs to 2.5 ± 0.3 in the PMCA2$^{+/-}$ PNs, $P < 0.05$, *t* test, $n = 12$. Similar reductions in the complex spike amplitude and the number of spikelets persisted in current clamp recordings from wild-type and PMCA2$^{+/-}$ PNs, $P < 0.05$, *t* tests, $n = 3$. Despite the fact that full voltage clamp of the CF-induced inward current in PNs is not possible and that spikelets also represent the activation of Na^+ (as well as Ca^{2+}) conductances (Llinás & Sugimori, 1980*a*,*b*; Schmolesky *et al.* 2002), the reduction in the complex spike and the spikelet number strongly suggested that CF-evoked calcium influx was reduced in PMCA2$^{+/-}$ PNs. Thus, the reduced amplitude of the $\%\Delta F/F$ CF-evoked calcium response in PMCA2$^{+/-}$ PNs can be explained, at least in part, by a reduced calcium influx.

Furthermore we noted slightly increased baseline fluorescence levels in PMCA2$^{+/-}$ PNs compared with PMCA2$^{+/+}$ PNs indicative of raised basal calcium levels, and this too probably contributed to the reduced peak $\%\Delta F/F$ values in PMCA2$^{+/-}$ PNs. Mean count values were $18{,}050 \pm 684$ in PMCA2$^{+/+}$ PNs ($n = 93$ dendrites), $20{,}013 \pm 626$ in PMCA2$^{+/-}$ PNs ($n = 126$ dendrites, $P = 0.03$, *t* test in a comparison between PMCA2$^{+/+}$ and PMCA2$^{+/-}$, arbitrary units) using similar laser intensities ($P = 0.8$, *t* test) and photomultiplier settings ($P = 0.11$, *t* test). Since we were also careful to control indicator levels in these experiments (see Methods) a rise in counts of approximately 10% in the PMCA2$^{+/-}$ PNs indicated a rise in basal levels of intracellular calcium. The *in vitro* K_d of OGB-1 in PNs is estimated to be 325 nM (Schmidt

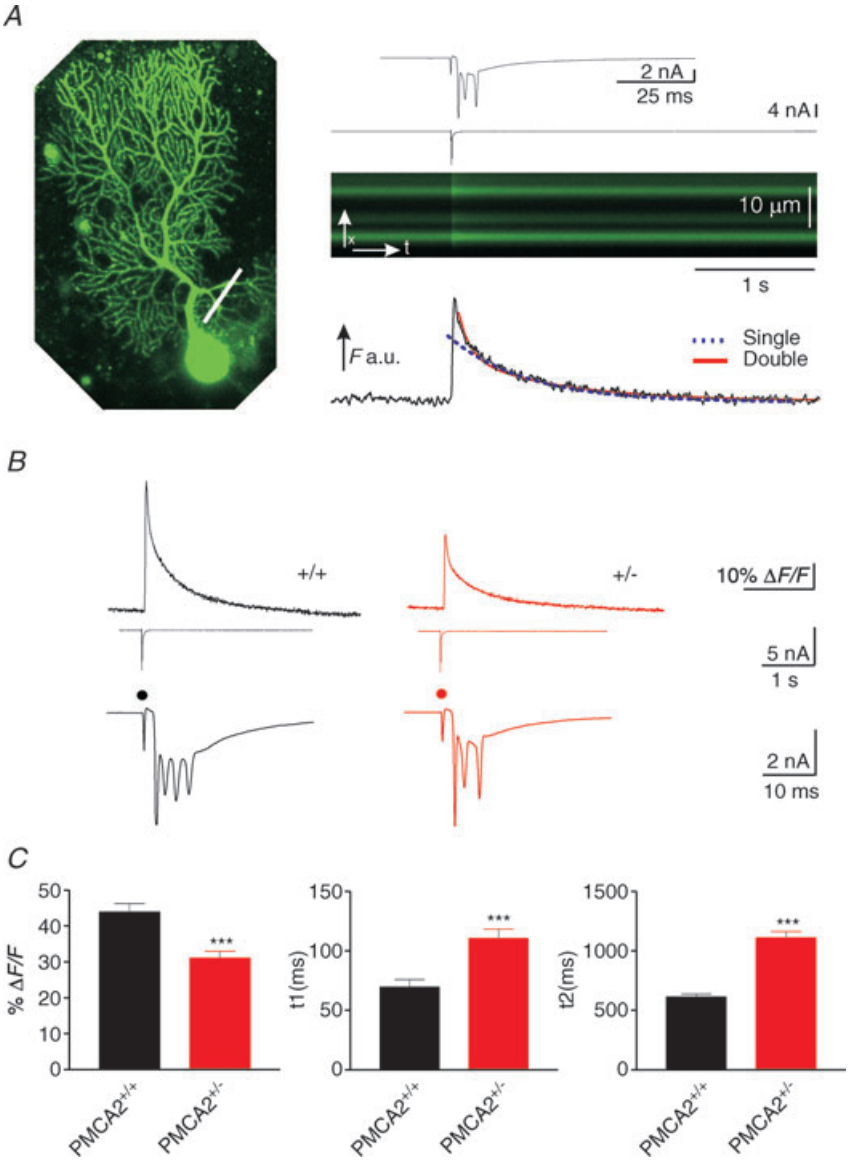

Figure 2. Climbing fibre-induced calcium transients and electrical responses were reduced in amplitude and the two phases of recovery of the calcium transient both slowed in PNs with reduced PMCA2 expression
A, PN from a PMCA2$^{+/-}$ mouse filled with 100 μM OGB-1 (left-hand panel) where a white bar indicates the approximate position of the linescan. The *x*–*t* plot of fluorescence change in response to CF activation is shown simultaneously with the electrophysiological voltage-clamp response (above, with the higher time resolution of the typical CF-induced inward current shown in the top panel). Below the *x*–*t* plot is the profile of the fluorescence (*F*; a.u., arbitrary units) change during the CF stimulation; note the sharp increase in fluorescence and its subsequent recovery, best fitted in the profile below, with a double exponential fit (continuous fitted line) compared with a single exponential fit (dashed line). *B*, average traces of fluorescence changes for all cells in the two different groups, showing the slowing of the recovery of the fluorescence-based calcium transient and the reduction in peak amplitude in the PMCA2$^{+/-}$ cells. Below each trace is a representative example of the CF response recorded in voltage-clamp mode, with the higher time resolution showing the repetitive spikes evoked in response to the climbing fibre stimulation. Note also the reduced number of spikelets superimposed upon the overall reduced inward current in the PMCA2$^{+/-}$ PN that is associated with the reduced peak amplitude of the calcium transient. Dot represents timing of application of climbing fibre stimulation. *C*, combined data for all cells. t1 and t2 represent the half-decay time of the first, fast, and second, slower phase of the fluorescence-based calcium transient. Error bars represent means ± S.E.M. ***Significance level at $P < 0.001$ (*t* test).

© 2010 The Authors. Journal compilation © 2010 The Physiological Society

et al. 2003) so a 10% increase in basal fluorescence reflects a rise in basal calcium levels of approximately 50 nM in PMCA2$^{+/-}$ PNs. This accords with results following partial inhibition of PMCA (using high pH) in superior cervical ganglion neurones where basal calcium rose from approximately 100 nM to approximately 200 nM (Wanaverbecq *et al.* 2003). The mild rise in basal calcium levels in PMCA2$^{+/-}$ PNs, in turn, might be the cause of the reduced amplitude of their CF-evoked calcium and inward current responses since voltage-gated P/Q channels in the PN membrane are inactivated in a calcium-dependent manner (Wykes *et al.* 2007). In order to test this possibility we recorded CF-evoked inward current responses with patch pipettes containing 10 mM EGTA to clamp basal intracellular calcium to low nanomolar levels (see Supplemental Fig. 1, available online only). Under these conditions the amplitude of the CF inward current and spikelet number in the PMCA2$^{+/-}$ PNs were rescued back to wild-type levels. This result indicates that the raised basal calcium in the PMCA2$^{+/-}$ cells was sufficient to reduce the amount of calcium entering the PN during CF activation so explaining the reduced amplitude of the CF-induced calcium transient.

Recovery of depolarization-induced dendritic calcium rises and calcium-dependent outward K$^+$ currents

We also used direct depolarization of the PN soma to stimulate rises in intracellular dendritic calcium levels. Under these conditions the fluorescence rises in PN dendrites were smaller than the CF-evoked transients (compare Figs 2 and 3, and see also Kano *et al.* 1995) but similarly recovered back to baseline with a biphasic decay best fitted with two exponentials (see Fig. 3*A*). As was the case for CF-induced calcium recovery, mean values of the first time constant were significantly prolonged in PMCA2$^{+/-}$ PN dendrites, from 136.5 ± 6.5 ms in wild-type ($n = 132$ dendrites from 7 cells) to 192 ± 11.7 ms in heterozygous PNs ($n = 114$ dendrites from 8 cells, $P < 0.0001$, *t* test). Likewise, as shown in Fig. 3*C*, the second component of the recovery of the depolarization-induced calcium transient was also significantly slowed when PMCA2 expression was reduced ($P < 0.0001$, *t* test); mean values were 595 ± 32 ms in wild-type and 1423 ± 73 ms in PMCA2$^{+/-}$, respectively. As for the CF-induced fluorescence responses above, the amplitude of the peak $\%\Delta F/F$ was also significantly reduced from $22 \pm 2.8\%$ in wild-type PNs to $11 \pm 1.2\%$ in PMCA2$^{+/-}$ PNs ($P < 0.0001$, *t* test). As seen in Fig. 3*B* this reduced peak calcium can be best explained by reduced calcium influx since the number of spikelets evoked during the depolarization step was also reduced in PMCA2$^{+/-}$ PNs. Mean values were 4.4 ± 0.6 spikelets in wild-type reduced to 3.5 ± 0.4 in PMCA2$^{+/-}$ cells ($P < 0.01$, *t* test).

Whilst it was important that our results from depolarization-induced calcium responses matched the CF data, the simultaneously recorded electrophysiological responses to depolarization provided some additional insights. Depolarization of PNs leads to calcium entry through their P/Q-type voltage-dependent calcium channels that then activates a slow Ca^{2+}-dependent K^+ channel-mediated outward current (Womack *et al.* 2004). As shown in Fig. 4, this outward current also recovered in a bi-exponential manner that closely matched the dual phase recovery of the depolarization-induced fluorescence-based calcium signal. The rate of the first, fast recovery of the current was slightly slower than the first, fast recovery of the fluorescence signal (compare Fig. 4*B* with Fig. 3*B*) in the wild-type PMCA2$^{+/+}$ control cells. The second phase of the current recovery was clearly longer than the time course of recovery of the fluorescence-based calcium signal and may represent the contribution of a calcium-independent component to the outward current. However, like the fluorescence-based calcium signal, both phases of the outward current were significantly slower in PMCA2$^{+/-}$ PNs compared with wild-type cells ($P < 0.001$, *t* test). This result was entirely consistent with the reduced expression of PMCA2 in the PMCA2$^{+/-}$ PNs leading to a slower calcium recovery that in turn prolonged this outward current.

Effects of pharmacological inhibition of PMCA activity

Thus far our results showed that half the PMCA2 expression in heterozygote PMCA2$^{+/-}$ PNs caused a near doubling in the time it took for peak calcium in the dendrites to recover, and that this relative accumulation of calcium also prolonged their depolarization-induced outward currents. To further validate these findings we wanted to exclude the possibility that our results arose from compensatory alterations to other proteins in PMCA2$^{+/-}$ PNs. To do this we treated wild-type PMCA2$^{+/+}$ PNs with 10 μM of the PMCA inhibitor carboxyeosin.

As shown in Fig. 5*A*, carboxyeosin treatment also slowed the recovery of the fluorescence-based calcium signal in PMCA2$^{+/+}$ PN dendrites in response to depolarization. The time course of both phases of recovery of the signal was significantly prolonged by carboxyeosin (see Fig. 5*B*), the mean values of the first and second time constants changing from 197 ± 19 to 303 ± 20 ms and from 1149 ± 90 to 2733 ± 444 ms, respectively ($P < 0.05$, paired *t* tests, $n = 20$ dendrites from 5 cells). The amplitude of the peak of the depolarization-induced fluorescence rise ($\Delta F/F$) was also reduced from $27.5 \pm 3.5\%$ to $18.6 \pm 3.7\%$ by carboxyeosin ($P < 0.05$, paired *t* test, $n = 20$). Carboxyeosin also slightly increased the baseline fluorescence, the mean values

© 2010 The Authors. Journal compilation © 2010 The Physiological Society

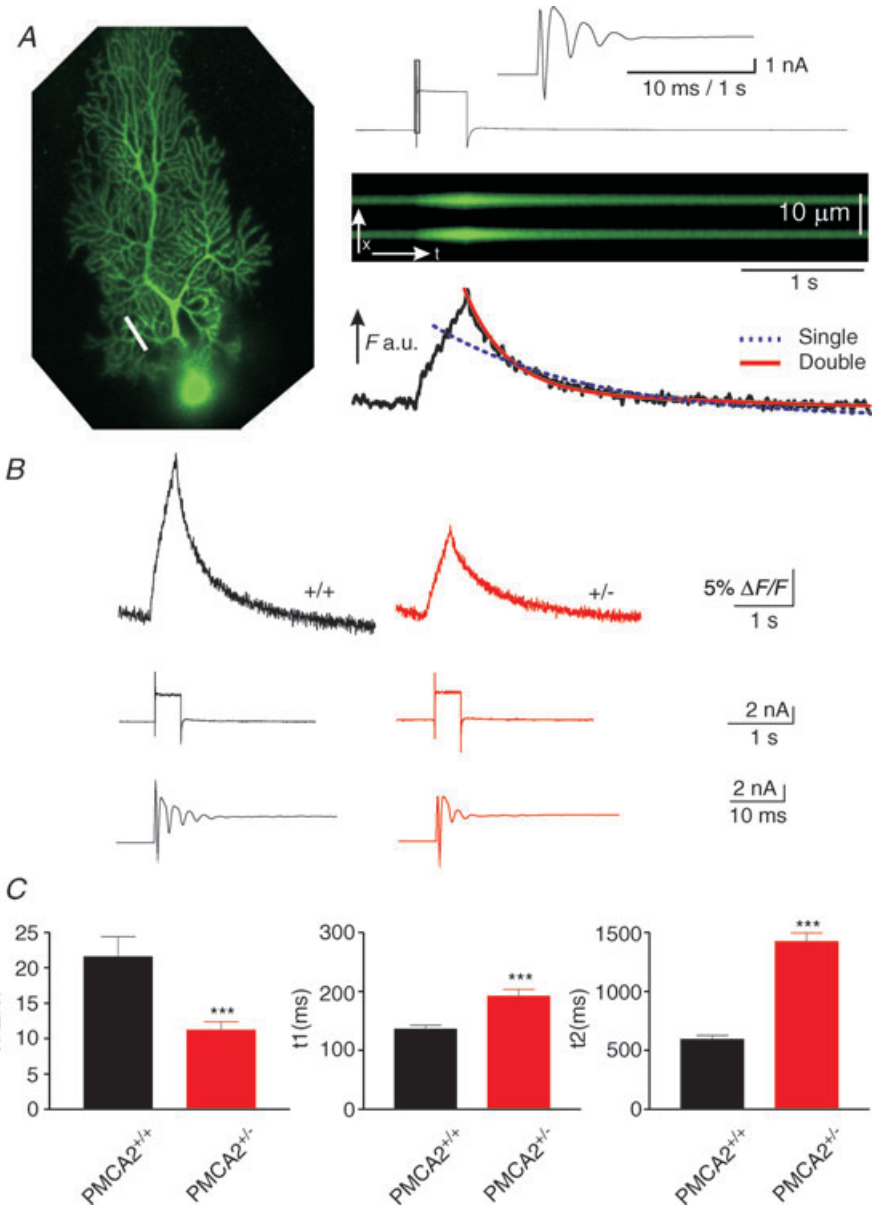

Figure 3. Depolarization-induced calcium transients and electrical responses were reduced in amplitude and the two phases of recovery of the calcium transient both slowed in PNs with reduced PMCA2 expression

A, PN from a PMCA2$^{+/-}$ mouse filled with 100 μM OGB-1 (left-hand panel) where a white bar indicates the approximate position of the linescan in the proximal PN dendrite. The *x*–*t* plot of fluorescence change in response to a 400 ms depolarization of the cell from −80 to 0 mV is shown simultaneously with the electrophysiological voltage-clamp response (above, with the higher time resolution of the early part of the depolarization response showing the spikelets in the top panel). Below the *x*–*t* plot is the profile of the fluorescence change during the depolarization; note the long and slow increase in fluorescence and its rapid curtailment as the membrane voltage is returned to −80 mV. The subsequent recovery of the calcium transient was best fitted in the profile below, with a double exponential fit (continuous fitted line) compared with a single exponential fit (dashed line). *B*, average traces of fluorescence changes for all cells in the two different groups, showing the slowing of the calcium transient and the reduction in their peak amplitudes. Below each trace is a representative example of the electrophysiological voltage-clamp response, with the higher time resolution showing the early response to depolarization for a representative cell. Note the reduced number of spikelets in the PMCA2$^{+/-}$ mice associated with the reduced peak amplitude of the calcium transient (right-hand traces). *C*, combined data for all cells. t1 and t2 represent the half-decay time of the first, fast, and second, slower phases of the fluorescence transient, both showing a progressive increase in decay time as PMCA2 expression is reduced. Error bars represent means ± S.E.M. ***Significance at $P < 0.001$ (*t* test).

© 2010 The Authors. Journal compilation © 2010 The Physiological Society

changing from 16,707 ± 1379 to 20,000 ± 987 counts ($n = 25$ dendrites from 4 cells, $P < 0.05$, paired t test). Presumably this occurred as a result of increased basal calcium, as we saw in the PMCA2$^{+/-}$ PNs, but may also have arisen from the fluorescent properties of carboxyeosin (Gatto & Milanick, 1993). It should be noted that an offset to the measured fluorescence level will underestimate the amplitude of the calcium signal but it will not by itself influence the time course of its recovery. Nevertheless, to further clarify the slowing of calcium recovery by carboxyeosin we took advantage of the fact that the time course of the depolarization-induced outward current will be sensitive to alterations in $[Ca^{2+}]_i$, but independent of changes in baseline fluorescence. As seen in Fig. 5*C*, the application of carboxyeosin significantly slowed both phases of the outward current, the mean values of its first and second time constants changing from 209 ± 9 ms and 889 ± 201 ms to 300 ± 36 ms and 1207 ± 361 ms, respectively, after carboxyeosin ($P < 0.05$, paired t tests $n = 5$ cells).

Carboxyeosin also slowed both recovery phases of the CF-induced fluorescence-based calcium transients and their amplitudes in PMCA2$^{+/+}$ PNs (Supplemental Fig. 2, available online only) and did not influence the number of CF-induced spikelets in wild-type cells filled with 10 mM EGTA when dendritic cytosolic calcium levels would be clamped to a very low level. Carboxyeosin also failed to alter either the first or second time courses of outward currents in PMCA2$^{-/-}$ PNs ($P = 0.35$ and 0.98, respectively, t tests, $n = 9$).

In summary, the close match between the carboxyeosin results and those from PMCA2$^{+/-}$ PNs confirmed the specificity of the observed effects of reduced PMCA2 expression in these cells.

Action potential firing frequency

Our findings therefore indicated that reduced PMCA2 activity in the PN directly slowed calcium extrusion leading to intracellular calcium accumulation, reduced peak calcium transients and a slowing of the recovery of calcium-dependent K^+ outward currents. Since all these findings would be consistent with reduced PN excitability we chose to use a non-invasive extracellular recording approach to determine if reduced expression of PMCA2 adversely affected PN spontaneous action potential firing. As shown in Fig. 6*A* the mean firing frequency

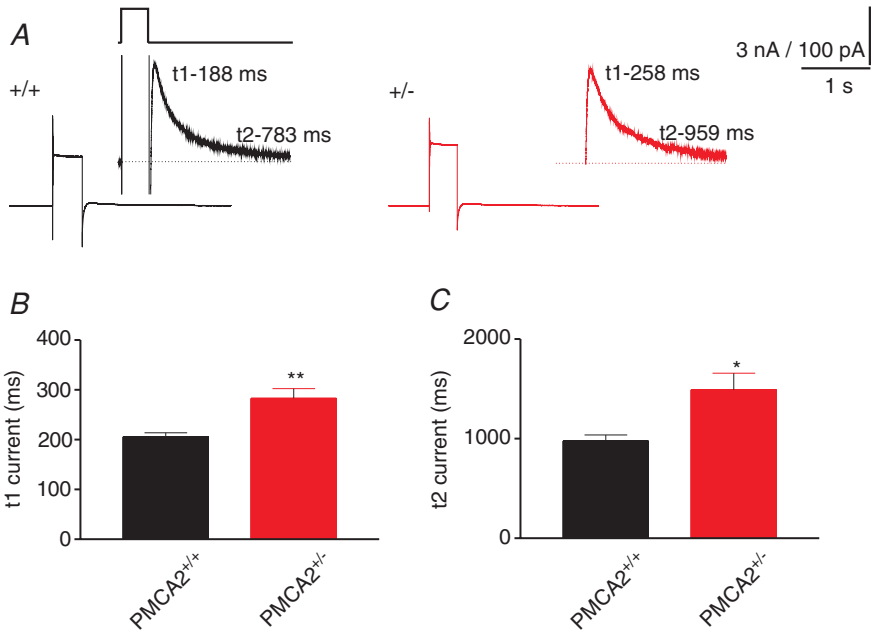

Figure 4. Depolarization-induced slow calcium-dependent outward currents decayed with two phases of recovery both of which were slowed in PNs with reduced PMCA2 expression
A, depolarization-induced currents for each of PCMA2$^{+/+}$ (left) and PMCA2$^{+/-}$ (right), in response to a depolarization from a holding potential of −80 to 0 mV for a duration of 400 ms before returning to −80 mV. The insets show the outward current observable at the end of the depolarizing pulse, shown in a representative manner by the upper thick black line. This current recovered to baseline in a manner best fitted with a double exponential. t1 and t2 numbers next to the trace indicate the first and second time constants for recovery for the trace shown. Traces are averages of at least 3 traces. Dotted lines represent the baseline current. *B* and *C*, combined data for all cells for t1 and t2, respectively, that represent the half-decay time of the first, fast, and second, slower phase of the recovery of the outward current, both showing an increase in decay time with reduced PMCA2 expression. Error bars represent means ± S.E.M. Significance levels: $^{**}P < 0.01$ and $^{*}P < 0.05$ (t test).

© 2010 The Authors. Journal compilation © 2010 The Physiological Society

of PNs was significantly reduced in the PMCA2$^{+/-}$ PNs compared with wild-type cells. The mean values were 7.4 ± 0.8 Hz ($n = 24$) compared with 15.8 ± 1.3 Hz ($n = 25$, $P < 0.001$, t test), although the distribution of instantaneous frequencies within both groups was similar (see Fig. 6*C*). The rather low firing frequency, compared with other reports (Häusser & Clark, 1997; Walter *et al.* 2006), was most likely a consequence of the room temperature of our recordings compared with the near physiological temperatures of others. Notwithstanding this difference, the comparably lower firing frequency in the PMCA2$^{+/-}$ PNs indicated a reduction of PN excitability associated with reduced PMCA2 expression and prolonged activation of calcium-dependent outward K^+ currents.

Motor performance

These clear alterations to PN action potential firing prompted us to examine more closely the motor performance of PMCA2$^{+/-}$ mice. We used two tests that can reveal subtle defects in motor coordination: footprint analysis with Catwalk and the ability of the mice to learn to cross a narrow, 1 cm wide, Plexiglas beam (Joho *et al.* 2004).

As shown in Fig. 7*A*, mice footprints looked very similar between the PMCA2$^{+/-}$ and PMCA2$^{+/+}$ mice indicating that on a flat surface the running behaviour of both sets of mice was very similar. (See online Supplemental Fig. 3 for a more detailed statistical comparison of gait parameters.) The lack of any significant alteration to their gait helps to

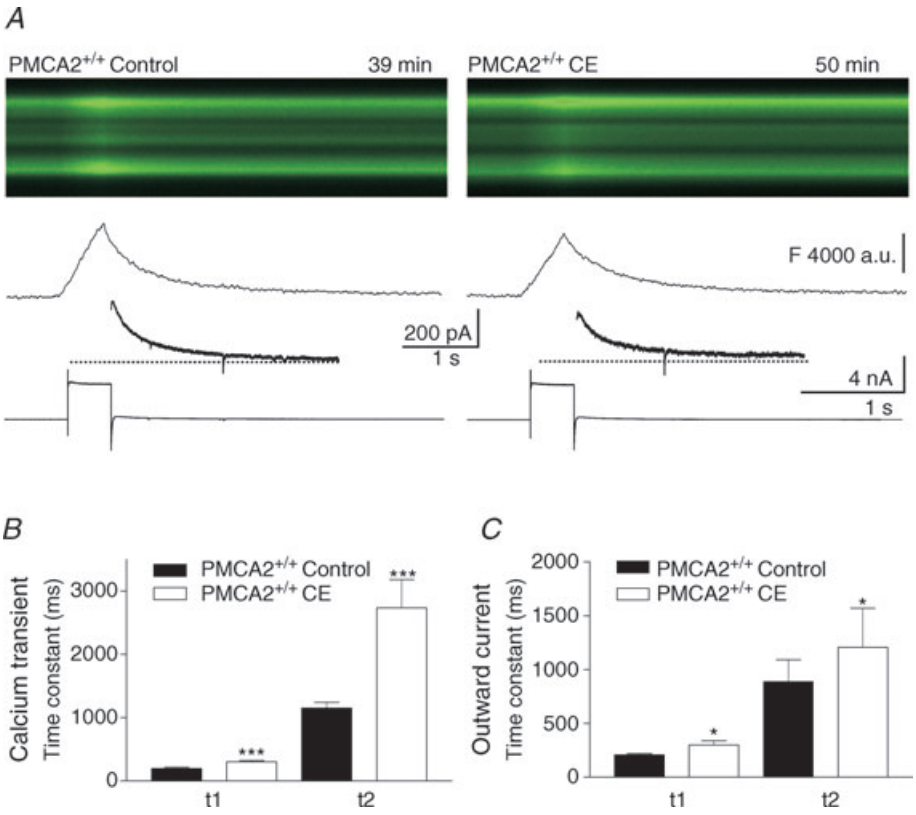

Figure 5. Carboxyeosin, a pharmacological inhibitor of PMCA slowed both phases of the recovery of depolarization-induced calcium transients and outward currents in PNs from PMCA2$^{+/+}$ mice
A, responses from a single PN before and after (left and right panels, respectively) treatment with 10 μM carboxyeosin (CE). The first *x–t* representation of the fluorescence-based calcium transient was recorded just before application of CE at 39 min after establishing the whole-cell patch-clamp configuration and the region of the dendrites was similar to the positions previously shown (e.g. Figs 2 and 3); the change in response in the same set of dendrites, following CE application, was recorded 11 min later, at 50 min. Below the *x–t* fluorescence traces the profile for the fluorescence change is shown, together with the outward current following the depolarization in the lower panel of each of the left and right panels. Dotted lines represent baseline current. *B* and *C*, combined data from all cells. *B* shows the change in both the fast and slow decay times of the calcium transient before and after CE (filled *versus* open bars) and *C* shows that the two phases of recovery of the outward current follow a similar pattern. Error bars represent means ± S.E.M. Significance levels: ***$P < 0.001$ and *$P < 0.05$ in paired t test comparisons before and after the application of CE.

© 2010 The Authors. Journal compilation © 2010 The Physiological Society

rule out spinal cord deficits in these mice (Hamers *et al.* 2006).

In contrast the more sensitive beam test (Barski *et al.* 2003; Joho *et al.* 2004), where the mice learn to place their feet accurately as they run along a 1 cm wide Plexiglas beam, did reveal clear differences between PMCA2$^{+/+}$ and PMCA2$^{+/-}$ mice. As the mice traversed the beam they made small slips with their hind- and forelimbs. The slips were not sufficient to cause any of the mice to fall from the beam, rather they quickly recovered their posture and continued running. As shown in Fig. 7*B*, left panel, one-month-old PMCA2$^{+/-}$ mice ($n = 14$) made significantly more hindlimb slips on the beam compared with their wild-type littermates ($P < 0.0001$ two-way ANOVA, $n = 8$), although both groups significantly improved their performance by making fewer slips throughout the 5 days of testing ($P < 0.0001$ two-way ANOVA). After a 2 day break both groups performed to their trained level on day 8 (see Fig. 7*B*) consistent with retention of improvements in motor performance. As shown in Fig. 7*B*, right panel, this level of motor skill was also retained for up to one month. Nevertheless, the PMCA2$^{+/-}$ mice always performed at a comparatively lower level than their wild-type littermates. Results from first time testing of 2-month-old mice showed a similar pattern to the 1-month-old mice with a clearly reduced performance of the PMCA2$^{+/-}$ mice compared with the PMCA2$^{+/+}$ mice ($P < 0.001$, two-way ANOVA, data not shown, $n = 4$ mice). As shown in Fig. 7*C*, both 1- and 2-month-old PMCA2$^{+/-}$ mice also took longer to cross the 1 m long beam compared with their littermate controls, and the younger mice were faster in all cases. Whilst the PMCA2$^{+/-}$ mice have recently been reported to exhibit mild reductions in motor unit estimates, their hind- and forelimb grip strength is normal (Souayah *et al.* 2008) and so too are their numbers of choline acetyl transferase-positive motor neurones (Kurnellas *et al.* 2005). Their vestibular apparatus is also normal although they do exhibit slightly impaired hearing (Kozel *et al.* 1998) as do heterozygous PMCA2 mutant *deafwaddler* mice (McCullough & Tempel, 2004).

Our behavioural analysis clearly demonstrated that PMCA2$^{+/-}$ mice exhibited a significant defect in motor performance. Importantly, the PMCA2$^{+/-}$ mice improved and retained their motor performance over days and weeks.

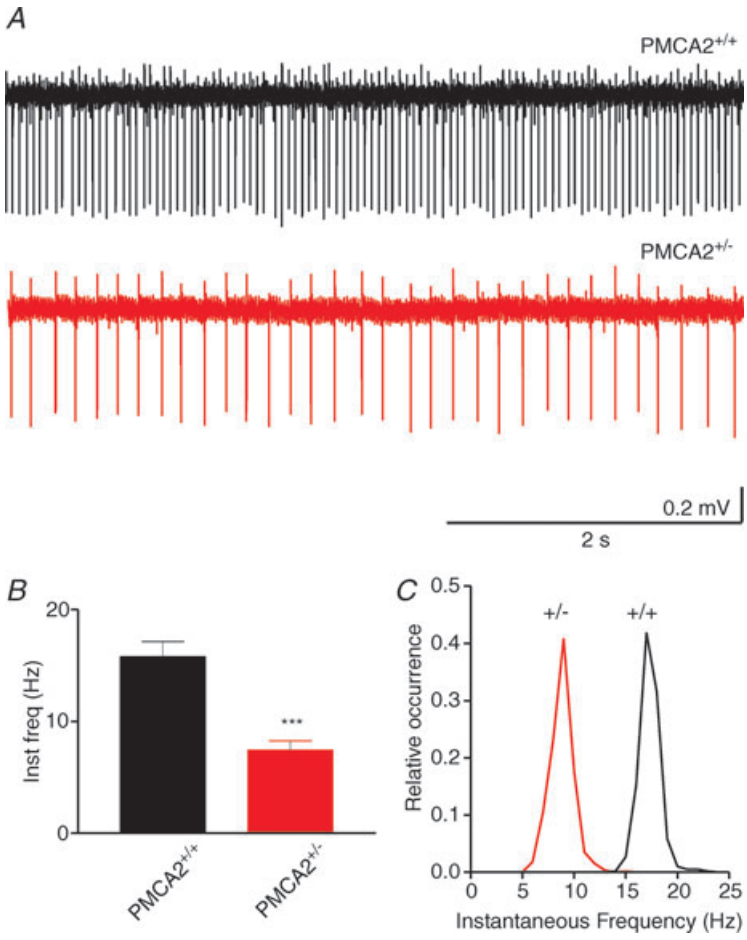

Figure 6. Reduced frequency of spontaneous action potential firing from PNs with reduced PMCA2 expression
A, representative traces from wild-type PMCA2$^{+/+}$ and heterozygous PMCA2$^{+/-}$ PNs where each spike event represents an extracellularly recorded action potential. Note that in all cells interspike intervals were irregular to some extent. In *B* the combined data for the mean instantaneous frequency (inst freq) in Hz is shown for all cells. ***Significance at $P < 0.001$ (*t* test). *C*, the distribution of instantaneous frequency for all cells in PMCA2$^{+/+}$ and PMCA2$^{+/-}$ groups indicate a similar spread of frequencies across the groups. Frequency values are binned at intervals of 1 Hz.

© 2010 The Authors. Journal compilation © 2010 The Physiological Society

Discussion

This study provides a body of evidence to show that PMCA2, a calcium 'off' mechanism in the cerebellum, is required for normal PN function and precise motor coordination in mice.

Contribution of PMCA2 to calcium clearance in Purkinje neurone dendrites

In PMCA2$^{+/-}$ mice, PMCA2 expression in the cerebellum was reduced, and in contrast to the PMCA2$^{-/-}$ mice, the gross structure of the cerebellum and the PNs were intact (Fig. 1). This provided an excellent opportunity to assess how PMCA2-mediated calcium clearance contributed to cerebellar PN physiology without complications from structural changes to the PMCA2$^{-/-}$ cerebellum (Kozel *et al.* 1998; Empson *et al.* 2007).

Stimulation of the CF input and somatic depolarization of PNs drives a transient rise in dendritic calcium of the order of several hundred nanomolar that then recovers in a bi-exponential manner through the combined action of fast and slow 'off' mechanisms (Schmidt *et al.* 2003; Hartmann & Konnerth, 2005). The halving of PMCA2 expression in the PMCA2$^{+/-}$ mice nearly doubled the time it took for PN calcium transients to recover. This and the mild rise in basal calcium levels indicated a very significant contribution of PMCA2 to calcium homeostasis in PN dendrites under normal conditions. Our result contrasts with previous results from PN soma where a pharmacological approach indicates that PMCAs contribute only 20% of calcium clearance (Fierro *et al.* 1998). The difference may reflect the greater need for a plasma membrane-located Ca^{2+} 'off' mechanism in the larger surface-to-volume ratio of PN dendrites, or a greater contribution in the soma from other 'off' mechanisms such as endogenous calcium buffers, SERCA (sarcoplasmic endoplasmic reticulum Ca^{2+}-ATPase) or the Na^+/Ca^{2+} exchanger (Hartmann & Konnerth, 2005).

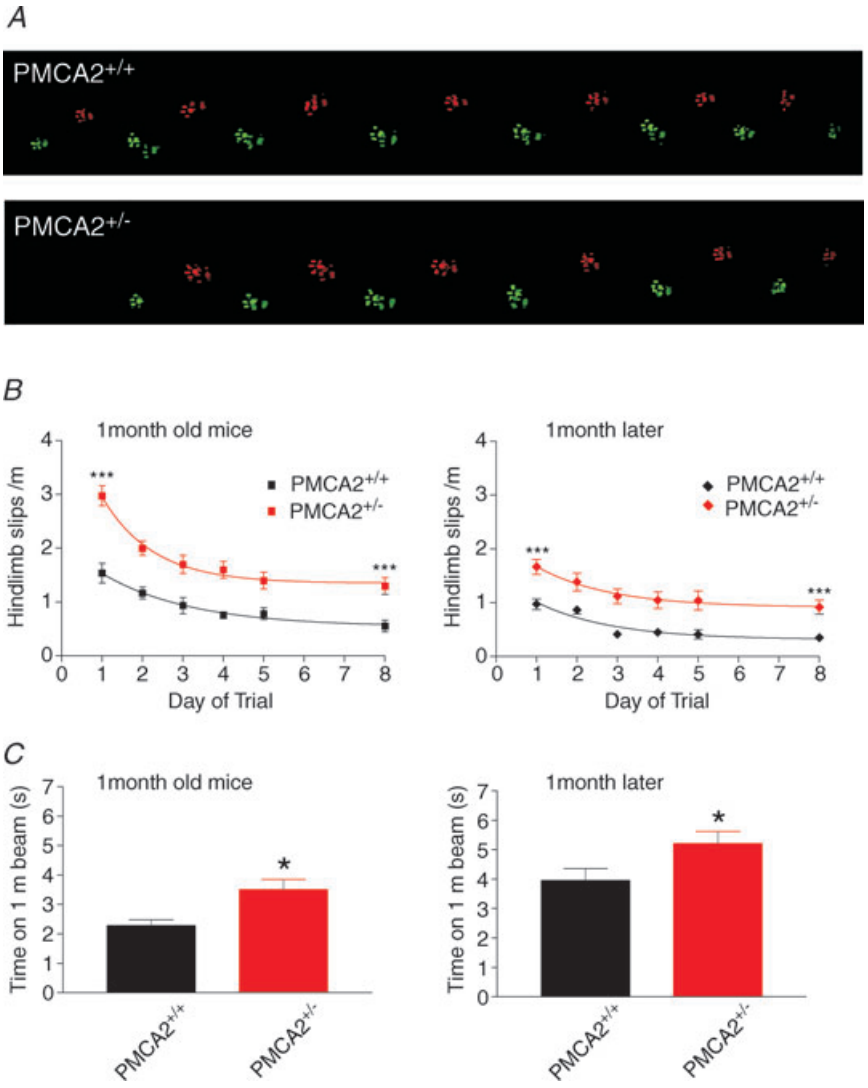

Figure 7. PMCA2$^{+/+}$ and PMCA2$^{+/-}$ mice displayed a similar walking gait but the PMCA2$^{+/-}$ mice performed poorly on the beam test
A, representative examples of footprint sequences from PMCA2$^{+/+}$ and PMCA2$^{+/-}$ mice, where red and green represent right and left prints respectively, with rear prints represented by the lighter shading. Note very little difference between the two mice. For a more detailed analysis of the gait parameters see online Supplemental Fig. 3. *B* shows that both young and pre-trained older mice negotiated a 1 m beam but exhibited a reduced number of hindlimb slips as they crossed the beam during daily trials over 1–8 days. PMCA2$^{+/-}$ mice (red symbols), however, performed less well making more slips throughout the training period. Error bars represent means ± S.E.M. Both data sets differed significantly in a two-way ANOVA revealing significant interactions at $P < 0.001$ (***) in terms of days of training within the groups and with respect to the two different genotypes. *C* shows the significantly slower time taken to traverse the beam by the PMCA2$^{+/-}$ mice in both the young, 1-month-old, and older, 2-month-old mice. Note the shorter crossing time in the young *versus* older PMCA2$^{+/+}$ mice. *Significance at $P < 0.05$ (*t* test).

© 2010 The Authors. Journal compilation © 2010 The Physiological Society

The 'fast' PMCA2a splice variant is enriched within the cerebellum (Filoteo *et al.* 1997) and was recently identified in PN dendrites and spines (Burette *et al.* 2009). Moreover, it is one of the most rapidly activating PMCAs (Caride *et al.* 2001; Brini *et al.* 2003) capable of responding to calcium levels in the tens of nanomolar range. More recent evidence shows cerebellar PMCA activity to be half-maximal at around 400 nM $[Ca^{2+}]$ (Berrocal *et al.* 2009), making it perfectly tuned to respond to the types of rises in calcium that accompany CF stimulation (Schmidt *et al.* 2003). In terms of kinetics, our results indicated that PMCA2 contributes to both phases of the PN calcium recovery (Figs 2 and 3). It is tempting to speculate that PMCA2a contributes to the early phase of recovery, whilst the slightly slower PMCA2b (Caride *et al.* 2001), also present in cerebellum (Filoteo *et al.* 1997), contributes to the later phase. However, endogenous calcium buffers are also a significant Ca^{2+} 'off' mechanism in PNs. The early phase of PN calcium recovery is attributed to calbindin (Airaksinen *et al.* 1997; Barski *et al.* 2003); while the slower phase is attributed to parvalbumin (Schmidt *et al.* 2003). However, as shown in Fig. 1*C*, calbindin levels were unchanged in the $PMCA2^{+/-}$ cerebellum, as were parvalbumin levels (P. R. Turner & R. M. Empson, unpublished observations), so this is unlikely to explain the slowing of calcium recovery in the $PMCA2^{+/-}$ PNs. More likely, our results reflect an altered interplay between the slightly slower, but active, PMCA2-driven calcium extrusion and the faster endogenous buffers (Aponte *et al.* 2008). At peak calcium a significant proportion of these high affinity calcium buffers in the PN will be saturated, but our results indicate that a fast, active extrusion mechanism like PMCA2 is ideally placed to make an important contribution. Firstly, as PMCA2 turns on, it will actively return calcium levels to a state where the buffers can release bound calcium and once this has happened it will continue to clear the calcium. Working in this way, the consequences of reduced PMCA2 activity would be a reduced calcium buffer capacity (since in its absence calcium would stay bound to parvalbumin and calbindin for longer), raised resting calcium levels and a slowing of both phases of the calcium recovery, all consistent with our findings. Furthermore, since PMCA2 is an active and modifiable enzymatic mechanism its ability to fine-tune calcium levels in a close relationship with the buffers could also influence calcium signalling dynamics under different physiological conditions (Ferragamo *et al.* 2009).

The consequences of reduced calcium clearance dynamics for Purkinje neurone excitability

A consequence of slowed calcium dynamics in the absence of PMCA2 was a prolonged activation of a depolarization-induced outward current (Fig. 5) that represents the activation of BK (large conductance) and SK (small conductance) calcium-dependent K^+ channels (Edgerton & Reinhart, 2003; Womack *et al.* 2004). This provided the first indication that the intrinsic excitability of PNs in the $PMCA2^{+/-}$ mice was adversely affected, especially as SK sets PN firing frequency (Edgerton & Reinhart, 2003). Non-invasive extracellular recordings revealed that spontaneous action potential firing frequency was significantly reduced in $PMCA2^{+/-}$ PNs, reminiscent of the reduced PN firing behaviour in ataxic *ducky* mutant mice (Donato *et al.* 2006) and in mice expressing the human FGF14 ataxia mutation (Shakkottai *et al.* 2009). Furthermore, reduced SK activation in PNs of EA2 mutant mice disrupts the regularity of PN action potential firing (Walter *et al.* 2006).

With kinetics that rely on intracellular $[Ca^{2+}]$ the depolarization-induced outward current also provided a useful, independent verification of our calcium measurements. Furthermore, pharmacological blockade of PMCA by carboxyeosin also prolonged the outward current and slowed calcium recovery in $PMCA2^{+/+}$ PNs. These results clearly demonstrated that slowed calcium and outward current recovery in $PMCA2^{+/-}$ PNs was a direct consequence of reduced PMCA2 expression and did not arise through 'compensatory' expression of other proteins.

A further consequence of reduced PMCA2 expression was the diminished CF-induced inward current in the $PMCA2^{+/-}$ PNs (Fig. 2) and the reduced amplitude of the peak calcium responses. These are likely to be a consequence of the increased basal calcium levels in response to loss of basal calcium turnover by PMCA2 in the PNs. Similarly, reduced PMCA activity raises basal calcium levels in peripheral neurones (Wanaverbecq *et al.* 2003) and cardiac myocytes (Choi & Eisner, 1999). In $PMCA2^{+/-}$ PNs, even slightly raised intracellular calcium levels would favour calcium-dependent inactivation of voltage-gated calcium channels. P/Q channels, as the main calcium entry route (or 'on' mechanism) for PN dendrites, are responsible, together with voltage-gated and persistent sodium currents, for the characteristic CF-induced spikelets of PNs (Llinás & Sugimori, 1980*a*,*b*; Schmolesky *et al.* 2002, but see also Davie *et al.* 2008). So enhanced inactivation of P/Q calcium channels (Wykes *et al.* 2007), precipitated by mildly elevated basal calcium in the $PMCA2^{+/-}$ PNs, provided a viable explanation for the reduced CF-induced inward current, reduced spikelets and reduced peak calcium responses in these cells. Furthermore, our ability to rescue the spikelets in $PMCA2^{+/-}$ PNs by heavily buffering intracellular calcium with EGTA supports this hypothesis. However, we cannot completely exclude a reduction in excitability of the $PMCA2^{+/-}$ Purkinje neurone dendrites or alterations to the voltage or calcium inactivation kinetics of their P/Q channels, as occurs following a *CACNA1A* mutation

© 2010 The Authors. Journal compilation © 2010 The Physiological Society

during late-onset ataxia in humans (Cuenca-León *et al.* 2009).

Motor performance deficits as a consequence of reduced calcium clearance from Purkinje neurones

Given the pivotal position of PNs within the cerebellar circuitry, the altered firing frequency and reduced CF responses in the PMCA2$^{+/-}$ PNs would be expected to impact on cerebellar function. Since a small reduction in the complex spike accompanies CF LTD, a phenomenon proposed to influence motor learning (Weber *et al.* 2003), the subtlety of changes to the PMCA2$^{+/-}$ PN excitability could be sufficient to disrupt cerebellar processing and motor performance (Ito, 2006). As shown in Fig. 7 the PMCA2$^{+/-}$ mice made far more hindlimb errors than their wild-type littermates when traversing a narrow beam (Crabbe *et al.* 2003; Barski *et al.* 2003; Joho *et al.* 2004). Importantly, training encouraged both sets of mice to cross the beam more accurately and they retained their improved skill level, but the PMCA2$^{+/-}$ mice were always the worst performers. Moreover, detailed assessment by Catwalk failed to reveal any gait deficits in the PMCA2$^{+/-}$ mice and suggests that their spinal cord function is intact (Hamers *et al.* 2006). Rather, defective cerebellar processing as a consequence of disrupted PN calcium dynamics seems the best explanation for the rather subtle behavioural deficits of the PMCA2$^{+/-}$ mice. Notably, our observations increase the number of examples where disrupted cerebellar signalling and motor performance were not associated with deficits in motor learning.

Together our results provide strong evidence that PMCA2 expression in Purkinje neurones is necessary to fine-tune their calcium and electrical signalling dynamics as a way to ensure accurate cerebellar processing.

References

Airaksinen MS, Eilers J, Garaschuk O, Thoenen H, Konnerth A & Meyer M (1997). Ataxia and altered dendritic calcium signalling in mice carrying a targeted null mutation of the calbindin D28k gene. *Proc Natl Acad Sci U S A* **94**, 1488–1493.

Aponte Y, Bischofberger J & Jonas P (2008). Efficient Ca^{2+} buffering in fast-spiking basket cells of rat hippocampus. *J Physiol* **586**, 2061–2075.

Barski JJ, Hartmann J, Rose CR, Hoebeek F, Mörl K, Noll-Hussong M, De Zeeuw CI, Konnerth A & Meyer M (2003). Calbindin in cerebellar Purkinje cells is a critical determinant of the precision of motor coordination. *J Neurosci* **23**, 3469–3477.

Berridge MJ, Bootman MD & Roderick HL (2003). Calcium signalling: dynamics, homeostasis and remodelling. *Nat Rev Mol Cell Biol* **4**, 517–529.

Berrocal M, Marcos D, Sepúlveda MR, Pérez M, Avila J & Mata AM (2009). Altered Ca^{2+} dependence of synaptosomal plasma membrane Ca^{2+}-ATPase in human brain affected by Alzheimer's disease. *FASEB J* **23**, 1826–1834.

Brini M, Coletto L, Pierobon N, Kraev N, Guerini D & Carafoli E (2003). A comparative functional analysis of plasma membrane Ca^{2+} pump isoforms in intact cells. *J Biol Chem* **278**, 24500–24508.

Burette AC, Rockwood JM, Strehler EE & Weinberg RJ (2003). Isoform-specific distribution of the plasma membrane Ca^{2+} ATPase in the rat brain. *J Comp Neurol* **467**, 464–476.

Burette AC, Strehler EE & Weinberg RJ (2009). "Fast" plasma membrane calcium pump PMCA2a concentrates in GABAergic terminals in the adult rat brain. *J Comp Neurol* **512**, 500–513.

Carafoli E (1992). The Ca^{2+} pump of the plasma membrane. *J Biol Chem* **67**, 2115–2118.

Caride AJ, Filoteo AG, Penheiter AR, Pászty K, Enyedi A & Penniston JT (2001). Delayed activation of the plasma membrane calcium pump by a sudden increase in Ca^{2+}: fast pumps reside in fast cells. *Cell Calcium* **30**, 49–57.

Choi HS & Eisner DA (1999). The role of sarcolemmal Ca^{2+}-ATPase in the regulation of resting calcium concentration in rat ventricular myocytes. *J Physiol* **515**, 109–118.

Crabbe JC, Metten P, Yu CH, Schlumbohm JP, Cameron AJ & Wahlsten D (2003). Genotypic differences in ethanol sensitivity in two tests of motor incoordination. *J Appl Physiol* **95**, 1338–1351.

Crepel F, Dupont JL & Gardette R (1984). Selective absence of calcium spikes in Purkinje cells of staggerer mutant mice in cerebellar slices maintained *in vitro*. *J Physiol* **346**, 111–125.

Cuenca-León E, Banchs I, Serra SA, Latorre P, Fernàndez-Castillo N, Corominas R, Valverde MA, Volpini V, Fernández-Fernández JM, Macaya A & Cormand B (2009). Late-onset episodic ataxia type 2 associated with a novel loss-of-function mutation in the *CACNA1A* gene. *J Neurol Sci* **280**, 10–14.

Davie JT, Clark BA & Häusser M (2008). The origin of the complex spike in cerebellar Purkinje cells. *J Neurosci* **28**, 7599–7609.

Donato R, Page KM, Koch D, Nieto-Rostro M, Foucault I, Davies A, Wilkinson T, Rees M, Edwards FA & Dolphin AC (2006). The ducky^{2J} mutation in *Cacna2d2* results in reduced spontaneous Purkinje cell activity and altered gene expression. *J Neurosci* **26**, 12576–12586.

Drummond GB (2009). Reporting ethical matters in *The Journal of Physiology*: standards and advice. *J Physiol* **587**, 713–719.

Eccles JC, Llinás R & Sasaki K (1966). The excitatory synaptic action of climbing fibres on the Purkinje cells of the cerebellum. *J Physiol* **182**, 268–296.

Edgerton JR & Reinhart PH (2003). Distinct contributions of small and large conductance Ca^{2+}-activated K^+ channels to rat Purkinje neurone function. *J Physiol* **548**, 53–69.

Eilers J, Augustine GJ & Konnerth A (1995). Subthreshold synaptic Ca^{2+} signalling in fine dendrites and spines of cerebellar Purkinje neurones. *Nature* **373**, 155–158.

© 2010 The Authors. Journal compilation © 2010 The Physiological Society

Empson RM, Garside M & Knöpfel T (2007). Plasma membrane Ca^{2+} ATPase 2 contributes to short-term synapse plasticity at the parallel fibre to Purkinje neurone synapse. *J Neurosci* **27**, 3753–3758.

Ferragamo MJ, Reinardy JL & Thayer SA (2009). Ca^{2+}-dependent, stimulus-specific modulation of the plasma membrane Ca^{2+} pump in hippocampal neurones. *J Neurophysiol* **101**, 2563–2571.

Fierro L, DiPolo R & Llano I (1998). Intracellular calcium clearance in Purkinje cell somata from rat cerebellar slices. *J Physiol* **510**, 499–512.

Filoteo AG, Elwess NL, Enyedi A, Caride A, Aung HH & Penniston JT (1997). Plasma membrane Ca^{2+} pump in rat brain. Patterns of alternative splices seen by isoform-specific antibodies. *J Biol Chem* **272**, 23741–23747.

Gatto C & Milanick MA (1993). Inhibition of the red blood cell calcium pump by eosin and other fluorescein analogues. *Am J Physiol Cell Physiol* **264**, C1577–C1586.

Hamers FP, Koopmans GC & Joosten EA (2006). CatWalk-assisted gait analysis in the assessment of spinal cord injury. *J Neurotrauma* **23**, 537–548.

Hansel C & Linden DJ (2000). Long-term depression of the cerebellar climbing fibre–Purkinje neurone synapse. *Neuron* **26**, 473–482.

Hartmann J & Konnerth A (2005). Determinants of postsynaptic Ca^{2+} signalling in Purkinje neurones. *Cell Calcium* **37**, 459–466.

Häusser M & Clark B (1997). Tonic synaptic inhibition modulates neuronal output pattern and spatiotemporal synaptic integration. *Neuron* **19**, 665–678.

Hu J, Qian J, Borisov O, Pan S, Li Y, Liu T, Deng L, Wannemacher K, Kurnellas M, Patterson C, Elkabes S & Li H (2006). Optimized proteomic analysis of a mouse model of cerebellar dysfunction using amine-specific isobaric tags. *Proteomics* **6**, 4321–4334.

Ito M (2006). Cerebellar circuitry as a neuronal machine. *Prog Neurobiol* **78**, 272–303.

Ito M & Kano M (1982). Long-lasting depression of parallel fibre–Purkinje cell transmission induced by conjunctive stimulation of parallel fibres and climbing fibres in the cerebellar cortex. *Neurosci Lett* **33**, 253–258.

Jensen TP, Filoteo AG, Knöpfel T & Empson RM (2007). Presynaptic plasma membrane Ca^{2+} ATPase isoform 2a regulates excitatory synaptic transmission in rat hippocampal CA3. *J Physiol* **579**, 85–99.

Joho RH, Street C, Matsushita S & Knöpfel T (2004). Behavioural motor dysfunction in Kv3-type potassium channel-deficient mice. *Genes Brain Behav* **5**, 472–482.

Kano M, Garaschuk O, Verkhratsky A & Konnerth A (1995). Ryanodine receptor-mediated intracellular calcium release in rat cerebellar Purkinje neurones. *J Physiol* **487**, 1–16.

Knöpfel T, Vranesic I, Staub C & Gähwiler BH (1991). Climbing fibre responses in olivo-cerebellar slice cultures. II. Dynamics of cytosolic calcium in Purkinje cells. *Eur J Neurosci* **3**, 343–348.

Kozel PJ, Friedman RA, Erway LC, Yamoah EN, Liu LH, Riddle T, Duffy JJ, Doetschman T, Miller ML, Cardell EL & Shull GE (1998). Balance and hearing deficits in mice with a null mutation in the gene encoding plasma membrane Ca^{2+}-ATPase isoform 2. *J Biol Chem* **273**, 18693–18696.

Kurnellas MP, Nicot A, Shull GE & Elkabes S (2005). Plasma membrane calcium ATPase deficiency causes neuronal pathology in the spinal cord: a potential mechanism for neurodegeneration in multiple sclerosis and spinal cord injury. *FASEB J* **19**, 298–300.

Lev-Ram V, Miyakawa H, Lasser-Ross N & Ross WN (1992). Calcium transients in cerebellar Purkinje neurons evoked by intracellular stimulation. *J Neurophysiol* **68**, 1167–1177.

Llinás R & Sugimori M (1980*a*). Electrophysiological properties of *in vitro* Purkinje cell dendrites in mammalian cerebellar slices. *J Physiol* **305**, 197–213.

Llinás R & Sugimori M (1980*b*). Electrophysiological properties of *in vitro* Purkinje cell somata in mammalian cerebellar slices. *J Physiol* **305**, 171–195.

McCullough BJ & Tempel BL (2004). Haplo-insufficiency revealed in deafwaddler mice when tested for hearing loss and ataxia. *Hear Res* **195**, 90–102.

McLennan IS & Taylor-Jeffs J (2004). The use of sodium lamps to brightly illuminate mouse houses during their dark phases. *Lab Anim* **38**, 384–392.

Miyakawa H, Lev-Ram V, Lasser-Ross N & Ross WN (1992). Calcium transients evoked by climbing fibre and parallel fibre synaptic inputs in guinea pig cerebellar Purkinje neurons. *J Neurophysiol* **68**, 1178–1189.

Schmidt H, Stiefel KM, Racay P, Schwaller B & Eilers J (2003). Mutational analysis of dendritic Ca^{2+} kinetics in rodent Purkinje cells: role of parvalbumin and calbindin D28k. *J Physiol* **551**, 13–32.

Schmolesky MT, Weber JT, De Zeeuw CI & Hansel C (2002). The making of a complex spike: ionic composition and plasticity. *Ann N Y Acad Sci* **978**, 359–390.

Shakkottai VG, Xiao M, Xu L, Wong M, Nerbonne JM, Ornitz DM & Yamada KA (2009). FGF14 regulates the intrinsic excitability of cerebellar Purkinje neurons. *Neurobiol Dis* **33**, 81–88.

Souayah N, Sharovetskaya A, Kurnellas MP, Myerson M, Deitch JS & Elkabes S (2008). Reductions in motor unit number estimates (MUNE) precede motor neuron loss in the plasma membrane calcium ATPase 2 (PMCA2)-heterozygous mice. *Exp Neurol* **214**, 341–346.

Strehler EE & Zacharias DA (2001). Role of alternative splicing in generating isoform diversity among plasma membrane calcium pumps. *Physiol Rev* **81**, 21–50.

Thayer SA, Usachev YM & Pottorf WJ (2002). Modulating Ca^{2+} clearance from neurons. *Front Biosci* **7**, d1255–d1279.

Walter JT, Alviña K, Womack MD, Chevez C & Khodakhah K (2006). Decreases in the precision of Purkinje cell pacemaking cause cerebellar dysfunction and ataxia. *Nat Neurosci* **9**, 389–397.

Wanaverbecq N, Marsh SJ, Al-Qatari M & Brown DA (2003). The plasma membrane calcium-ATPase as a major mechanism for intracellular calcium regulation in neurones from the rat superior cervical ganglion. *J Physiol* **550**, 83–101.

Weber JT, De Zeeuw CI, Linden DJ & Hansel C (2003). Long-term depression of climbing fibre-evoked calcium transients in Purkinje cell dendrites. *Proc Natl Acad Sci U S A* **100**, 2878–2883.

© 2010 The Authors. Journal compilation © 2010 The Physiological Society

Womack MD, Chevez C & Khodakhah K (2004). Calcium-activated potassium channels are selectively coupled to P/Q-type calcium channels in cerebellar Purkinje neurons. *J Neurosci* **24**, 8818–8822.

Wykes RC, Bauer CS, Khan SU, Weiss JL & Seward EP (2007). Differential regulation of endogenous N- and P/Q-type Ca^{2+} channel inactivation by Ca^{2+}/calmodulin impacts on their ability to support exocytosis in chromaffin cells. *J Neurosci* **27**, 5236–5248.

Author contributions

Simultaneous calcium imaging and electrophysiology experiments were conducted at RIKEN, immunohistochemistry, western blotting, electrophysiology and behaviour were conducted at the University of Otago. R.M.E. and T.K. were responsible for the concept, design, experimentation, analysis and interpretation of data and writing and critically revising the manuscript; P.R.T. and R.Y.N. contributed to the concept, experimentation and analysis and interpretation of data and manuscript revision; P.W.B. contributed to the concept and manuscript revision. All authors approved the final published version.

Acknowledgements

We acknowledge the support of an HRC-JSPS (Health Research Council–Japanese Society for the Promotion of Science) fellowship to R.M.E. and other funding from the Neurological Foundation of New Zealand, The Division of Health Sciences and Department of Physiology, University of Otago and RIKEN intramural funding to T.K.

© 2010 The Authors. Journal compilation © 2010 The Physiological Society